

**IGF-I GENE THERAPY IN AGING RATS MODULATES HIPPOCAMPAL GENES RELEVANT TO
MEMORY FUNCTION**

Joaquín **Pardo**¹, Martin **C. Abba**², Ezequiel **Lacunza**², Olalekan M. **Ogundele**³, Isabel **Paiva**⁴,
Gustavo R. **Morel**^{1*}, Tiago F. **Outeiro**^{4,5*}, Rodolfo G. **Goya**^{1*}

¹INIBIOLP-Histology B-Pathology B; ²CINIBA, School of Medicine, UNLP, La Plata, Argentina; ³Department of Comparative Biomedical Sciences, Louisiana State University, School of Vet. Medicine, Baton Rouge, USA; ⁴Department of Experimental Neurodegeneration, Center for Nanoscale Microscopy and Molecular Physiology of the Brain, Center for Biostructural Imaging of Neurodegeneration, University Medical Center Göttingen, Göttingen, Germany; ⁵Max Planck Institute for Experimental Medicine, Göttingen, Germany.

Send correspondence and reprint requests to:

Rodolfo Goya,

INIBIOLP, Faculty of Medicine, UNLP,

CC 455 ;

(zip 1900) La Plata,

Argentina

Telephone: (54-221)425-6735; Fax: (54-221) 425-0924 ;

E-mail: goya@isis.unlp.edu.ar

* These authors contributed equally to this work.

© The Author 2017. Published by Oxford University Press on behalf of The Gerontological Society of America. All rights reserved. For permissions, please e-mail: journals.permissions@oup.com.

Running title: IGF-I and hippocampal transcriptome in old rats

Keywords: aging – IGF-I - spatial memory – hippocampal transcriptome - Barnes maze

ABSTRACT

In rats, learning and memory performance decline during normal aging, which makes this rodent species a suitable model to evaluate therapeutic strategies. In aging rats, insulin-like growth factor-I (IGF-I), is known to significantly improve spatial memory accuracy as compared to control counterparts. A constellation of gene expression changes underlie the hippocampal phenotype of aging but no studies on the effects of IGF-I on the hippocampal transcriptome of old rodents have been documented. Here, we assessed the effects of IGF-I gene therapy on spatial memory performance in old female rats and compared them with changes in the hippocampal transcriptome. In the Barnes maze test, experimental rats showed a significantly higher exploratory frequency of the goal hole than controls. Hippocampal RNA-sequencing showed that 219 genes are differentially expressed in 28 months old rats intracerebroventricularly injected with an adenovector expressing rat IGF-I as compared with placebo adenovector-injected counterparts. From the differentially expressed genes, 81 were down and 138 upregulated. From those genes, a list of functionally relevant genes, concerning hippocampal IGF-I expression, synaptic plasticity as well as neuronal function was identified. Our results provide an initial glimpse at the molecular mechanisms underlying the neuroprotective actions of IGF-I in the aging brain.

INTRODUCTION

In humans and rats, brain aging is associated with a progressive deterioration of spatial learning and memory, which makes this rodent species a suitable model to evaluate therapeutic strategies of potential value for correcting age-related cognitive deficits. Some of these strategies involve the administration of neurotrophic factors, one of which, insulin-like growth factor-I (IGF-I), is emerging as a promising molecule that plays a physiologic role in neuroprotection. Intracerebroventricular (ICV) infusion of IGF-I in the lateral ventricles improves reference and working memory in aging rats **(1)**. Also, it has been documented that IGF-I protects hippocampal neurons from the toxic effects of amyloid peptides **(2)**. Furthermore, IGF-I treatment markedly reduced the brain burden of A β amyloid in transgenic mice expressing a mutant A β amyloid peptide **(3)**.

Gene therapy for IGF-I in the central nervous system (CNS) of senile rats has shown promising results. Thus, a recombinant adenoviral vector (RAV) harboring the gene for rat IGF-I was used to implement IGF-I gene therapy in the hypothalamus of aging female rats displaying tuberoinfundibular dopaminergic neurodegeneration and chronic hyperprolactinemia. The treatment reversed hyperprolactinemia and increased the number of dopaminergic neurons in

the hypothalamus of the aging rats (4). The ependymal route is particularly suitable for RAD-mediated gene delivery as it can effectively increase IGF-I levels in the cerebrospinal fluid (CSF) of rats (5). Taking advantage of this fact, we performed ICV IGF-I gene therapy in very old female rats and achieved a significant amelioration of their motor performance (6). In aging rats, it has been recently shown that IGF-I gene therapy significantly improves spatial memory accuracy as compared to control counterparts. Furthermore, in the dentate gyrus (DG) of the old rats submitted to IGF-I gene therapy there was a higher number of immature neurons than in the old controls (7).

There is clear evidence that a constellation of gene expression changes underlie the hippocampal phenotype of aging. Thus, gene expression studies in aging rodents have documented significant changes in hippocampal genes related to cholesterol synthesis, inflammation, transcription factors, neurogenesis and synaptic plasticity (8-12). While those studies revealed that aging itself is associated with the majority of gene expression changes, a smaller portion of the transcriptional differences in the hippocampus are related to changes in learning and spatial memory performance. The above evidence prompted us to assess the effect of ICV IGF-I gene delivery on the hippocampal transcriptome in old rats compared with placebo vector-treated counterparts.

MATERIALS AND METHODS

Animals

Twenty three 25-months old female Sprague-Dawley rats weighing 267 ± 5 g were used. Rats were housed in a temperature-controlled room ($22 \pm 2^{\circ}\text{C}$) on a 12:12 h light/dark cycle. Food and water were available *ad libitum*. We used a commercial diet whose percentual composition was: humidity, 12%; protein, 23%; lipids, 7%; raw fiber, 6%; Total minerals, 10%,

Ca, between 1.0 and 1.4%; P, between, 0.5 and 0.8%; Cl, 0.3%; Na, 0.2%; K, 0.7%; Mg, 0.2%; S, 0.16%. All experiments with animals were performed in accordance to the Animal Welfare Guidelines of NIH (INIBIOLP's Animal Welfare Assurance No A5647-01). The ethical acceptability of the animal protocols used in this study was approved by our institutional IACUC (Protocol # T09-01-2013).

Spatial memory assessment

The modified Barnes maze protocol used here has been previously documented (7,13). It consists of an elevated (108 cm to the floor) black acrylic circular platform, 122 cm in diameter, containing twenty holes around the periphery. The holes are of uniform diameter (10 cm) and appearance, but only one hole is connected to a black escape box (tunnel). The escape box is 38.7 cm long x 12.1 cm wide x 14.2 cm in depth and it is removable. A white cylindrical starting chamber (an opaque, 25 cm in diameter and 20 cm high, open-ended chamber) is used to place rats on the platform with a random orientation of their bodies.

Four proximal visual cues are placed in the room, 50 cm away from the circular platform. The escape hole is numbered as hole 0 for graphical normalized representation purposes, the remaining holes being numbered 1 to 10 clockwise, and -1 to -9 counterclockwise. During the whole experiment, hole 0 remained in a fixed position, relative to the cues in order to avoid randomization of the relative position of the escape box. A 90-dB white-noise generator and a white-light 500 W bulb provided the escape stimulus from the platform. At the beginning of the experiment, rats were habituated to the task. The habituation routine consists of placing the animals in the starting chamber and escape box during 180 s. The purpose of habituation

consists of accustoming animals to new environments and lowers the level of anxiety. An acquisition trial (AT) consists of placing a rat in the starting chamber, located at the center of the platform, for 30 s; the chamber is then raised, the aversive stimuli (bright light and high pitch noise) are switched on and the rat is allowed to freely explore the maze for 120 s. The purpose of ATs is to train the rats on finding the escape hole. A probe trial (PT) is similar to an AT except that the escape box has been removed, the purpose being to assess recent spatial memory retention. During PTs, rats explore the maze for 90 s. The behavioral performances were recorded using a computer-linked video camera mounted 110 cm above the platform. The performance of the subjects was determined using the Kinovea v0.7.6 (<http://www.kinovea.org>) software. The behavioral parameters assessed were as follows.

(a) Escape box latency: time (in s) spent by an animal since its release from the starting chamber until it enters the escape box (during an AT) or until the first exploration of the escape hole (during a PT). A shorter escape box latency time indicates a better learning.

(b) Nongoal hole exploration (errors): number of explorations of holes different from the escape one. Each exploration of an incorrect hole is counted as an error, provided that the rat lowers its nose below the plane of the table surface.

(c) Exploration frequency: the times the rat explores every hole of the maze during the allotted time (90 s). A higher exploration frequency of the goal hole and the holes close to it indicates higher spatial memory accuracy.

Helper-dependent adenovectors (HD-RAd)

HD-RAds were constructed using a kit sold by Microbix Biosystems (Ontario, Canada). The kit provides the shuttle plasmid pC4HSU, the helper virus H14 and the 293 Cre4 cell line. The

construction procedure followed the guidelines of the Microbix manual and those described by Oka and Chan (14). Briefly, an expression cassette containing the gene for either rat IGF-I or the red fluorescent protein DsRed, both under the control of the murine cytomegalovirus (mCMV) promoter, was cloned in pC4HSU, a plasmid that consists of the ITRs for Ad 5 virus, the packaging signal and part of the E4 adenoviral region plus a stuffer noncoding DNA of human origin which keeps a suitable size (28-31 Kbp) of the viral DNA so that it is efficiently packaged into the capsids during vector generation but bands at sufficient distance from helper virus H14 in CsCl gradients, thus minimizing the risk of contamination of the newly generated vector. The shuttle vector harboring the expression cassette of interest was transfected in 293 Cre4 cells which were then infected with the helper virus Ad H14 whose packaging signal is flanked by lox P sites recognized by the Cre recombinase expressed by the 293 Cre4 cells. Therefore, the helper virus provides in trans all of the viral products necessary for generation of the desired HD-RAd. Following iterated coinfections with the HD-RAd and H14 virus, a sufficiently high concentration of HD-RAd is generated whereas very low levels of H14 are produced due to the cleavage of the packaging signal of H14 effected by the Cre recombinase. The new adenovectors, termed **HD-RAd-IGF-I** and **HD-RAd-DsRed** as appropriate, were purified by ultracentrifugation in a CsCl gradient and titrated for adenoviral particles.

Experimental design

We used a modified version of the protocol for the Barnes maze paradigm already described in our laboratory (7, 13). On experimental day -10 the animals were habituated as described above. The task was organized into 3 separate sessions at one month interval. Every session lasted 9 days and consisted of four ATs per day, done every fifteen minutes. On the last day of

each session, fifteen minutes after the last AT a PT was conducted to assess spatial memory as preference for the goal hole (hole 0). On experimental day -10, ten rats were allotted to group “DsRed” (injected with placebo Adenovirus) and 12 rats were allotted to group “IGF-I” (injected with an IGF-I Adenovirus) (see below). On experimental day 0 rats were ICV injected with the IGF-I or DsRed vector as appropriate and on day 80, CSF was obtained from the great cerebral cistern by puncture as previously documented (6). On experimental day 80, at age 28 months, animals were euthanized by rapid decapitation and their hippocampi microdissected and stored at -80°C until RNA extraction (see below) (Fig 1A).

Stereotaxic injections. DsRed and IGF-I rats were anesthetized with ketamine hydrochloride (40 mg/kg; ip) plus xylazine (8 mg/kg; im) and placed in a stereotaxic apparatus. In order to access the lateral ventricles (LV), the tip of a 26G needle fitted to a 10µl syringe was placed at the following coordinates relative to the bregma: -0.8 mm anteroposterior, 4.1 mm dorsoventral and ±1.5 mm mediolateral (15). The animals were injected bilaterally with 8 µl per side of a suspension containing 1.7×10^{12} viral particles of the appropriate vector.

IGF-I assay. IGF-I was extracted from CSF samples (20 µl) by acid-ethanol cryoprecipitation and was radioimmunoassayed using antibody UB2-495 from L. Underwood and J.J. Van Wyk, which is distributed by the Hormone Distribution Program of the National institute of Diabetes and Digestive and Kidney diseases (NIDDK, Bethesda), National Hormone and Pituitary Program. Recombinant human IGF-I (rh IGF-I, Chiron Corp., Emeryville, CA) was used as tracer and unlabeled ligand. Intra and inter-assay coefficients of variation were 7.2 and 12.8%, respectively.

RNA extraction, library preparation, and sequencing

The brains from four rats per group (i.e., DsRed and IGF-I groups) were rapidly removed after euthanasia and their right hippocampus dissected for transcriptome analysis. The hippocampus was stored at -80°C until RNA extraction.

Tissues were homogenized in TRIzol Reagent (Life Technologies). The quality of the isolated RNA was assessed by measuring the RIN (RNA Integrity Number) using the Fragment Analyzer. Library preparation for RNA-Seq was performed using the truSeq RNA Sample Preparation Kit (Illumina, Cat. N° RS-122-2002) starting from 500 ng of total RNA. Accurate quantitation of cDNA libraries was performed using the QuantiFluor™ dsDNA System (Promega). The size range of final cDNA libraries was 280-320 bp and was determined applying the DNA Chip for NGS Libraries using the Fragment Analyzer (Advanced Analytical). cDNA libraries were amplified and sequenced by using the cBot and HiSeq2000 from Illumina (SR; 50 bp; ca. 30–35 million reads per sample). Raw datasets have been submitted to NCBI GEO database.

All original transcriptome data were deposited in the NCBI's Gene Expression Omnibus (RNA-seq, GEO number: GSE100021).

RNA-Seq data analysis

Illumina HiSeq 2000 fluorescence images were transformed to BCL files with the Illumina BaseCaller software and samples were demultiplexed to FASTQ files with CASAVA (version 1.8.2). Sequencing quality was checked and approved via the FastQC software. Sequences were aligned to the genome reference sequence of *Rattus norvegicus* (RGSC assembly v5.0) using the STAR alignment software **(16)** allowing for 2 mismatches within 50 bases. Subsequently, resulting SAM files were converted to sorted BAM files, filtering of unique hits and counting was conducted with SAM tools **(17)** and HTSeq **(18)**.

We used the Bioconductor package edgeR for differential expression analysis of reads counts arising from RNAseq between hippocampal samples from IGF-I and DsRed rats. **(19)**. The list of

differentially expressed genes (DEG) was established from a Log Fold Change > 0.5 and a p adj. value <0.05.

Functional enrichment analyses of DEG were performed using the databases for annotation, visualization and integrated discovery (DAVID, <http://david.abcc.ncifcrf.gov/>), Enrichr (<http://amp.pharm.mssm.edu/Enrichr/>), and GeneMania resources (<http://genemania.org/>). Data integration and plots visualization were done with R and the MultiExperiment Viewer software (MeV v4.9) (20).

Q RT-PCR

Total RNA was treated with gDNA wipeout and cDNA was synthesized with the Qiagen QuantiTect Reverse transcription kit (#205310). qPCR was performed with the MESA BLUE qPCR MasterMix Plus for SYBR Assay Low ROX on a Stratagene Mx3000P qPCR system. The primers used are listed in **Suppl Table 1**. The $2^{(-\Delta\Delta_{CT})}$ method was employed for measuring the gene variation between DsRed and IGF-I rats.

Statistics

Behavioral data were analyzed with the GraphPad Prism 6 Software. Latency to escape box and errors made were analyzed by Two way ANOVA, considering AT and treatment factors. When ANOVA was significant, comparisons between means and AT1 were performed with the Sidak post hoc test. Unpaired t-test was used for IGF-I levels, goal hole exploration in PTs and qRT-PCR. For RNAseq data analysis, as described above, we used the statistical language R and the analysis packages from Bioconductor.

RESULTS

Effects of IGF-I gene therapy on spatial memory

Latency and errors to escape box. The treatment did not induce significant changes in either latency or errors to escape box, two parameters that are a measure of learning ability. During the first series of AT sessions, (before treatment), both parameters fell significantly at comparable rates in the two groups (Two way ANOVA, Treatment factor $p=0.19$, AT factor $p<0.0001$, interaction $p=0.34$) (Sidak post-hoc test AT2 onwards vs AT1 $p<0.0001$). During sessions 2 and 3 both latency and errors to escape box remained low in both groups, indicating that the animals remembered the location of the escape hole as well as at the end of session 1 (**Fig. 1B&C**).

Hole exploration frequency. As expected, hole exploration frequency showed overlapping bell-shaped distributions around hole 0 in the pre-treatment PT (**Fig. 1D**). Thirty-eight days after vector injection the distribution of exploration frequency remained comparable in both groups (**Fig. 1E**), but at 77 days post-treatment, exploration frequency of the goal hole (hole 0) in the IGF-I group was significantly higher than in the DsRed counterparts (unpaired t-test $t=2,644$, $df=20$, $p=0.016$). (**Fig. 1F**). The higher exploration frequency displayed in PT3 by the IGF-I rats at the goal hole suggests that at this time point, the treatment increased the accuracy of spatial memory in the aged animals.

Ventricular transgene expression and IGF-I levels

Two days after ICV DsRed adenovector injection there was a strong expression of DsRed in the ependymal cells lining the cerebral ventricles (**Fig 2A, B, C and D**). Eighty days after vector injection (on the day of sacrifice) transgene expression in the ependymal cell layer was still

observable (**Fig 2E, F and G**). On experimental day 80 CSF levels of IGF-I were significantly higher in the IGF-I group than in the DsRed counterparts (unpaired t-test $t=4.967$, $df=5$, $p=0.0042$) (**Fig 2H**). The results of this section indicate that transgene expression of the adenovector genome in the ependymal cells remains active for at least 80 days after injection.

Hippocampal genes whose expression is modified by IGF-I gene therapy in old rats

Analysis of the hippocampal transcriptome of old rats revealed that after long-term IGF-I gene therapy, 219 genes were significantly ($P<0.05$) differentially expressed, 81 down and 138 up (**Suppl table 2**). We performed quantitative RT-PCR analysis of 4 representative transcripts namely, *Itga 8*, *Sypl2*, *Dusp1* and *Nnat*. The results were in line with the RNAseq data (**Fig 3D**).

From those genes, a list of functionally relevant genes, concerning hippocampal IGF-I expression, synaptic plasticity as well as neuronal function was identified (**Table 1**). They were grouped as follows.

Hippocampal genes related to IGF-I expression and transport- Expression of IGF-I and its binding protein IGFBP-6, in the hippocampus was significantly upregulated by ICV IGF-I gene therapy. In contrast, the treatment downregulated the expression of the gene encoding IGF binding protein IGFBP-4. Data analysis using the Kyoto Encyclopedia of Genes and Genomes (KEGG) database collections revealed that the IGF-I gene is functionally linked to a number of metabolic pathways and to several of the hippocampal genes differentially expressed by the treatment (**Fig. 3**).

Genes involved in synaptic plasticity and neurogenesis- Three genes related with synaptic processes were up-regulated after IGF-I gene therapy. The up-regulated genes were Synaptophysin-like protein 2 (*Sypl2*), Neuronatin (*Nnat*) and integrin $\alpha 8$ subunit (*Itga-8*). *Sypl2* is an integral component of synaptic vesicle membrane, cellular calcium ion homeostasis,

transporter activity and substantia nigra development (see the Discussion section for further details).

Nnat mRNA is abundant in dendrites particularly in rat brain embryos.

ITGA8 expression in brain mediates cell-cell interactions and regulates neurite outgrowth of sensory and motor neurons. The neurogenesis related gene DCX, that encodes the cytoskeletal protein doublecortin, was significantly upregulated by the treatment.

Micro RNA 186 (miRNA 186) and β -site amyloid precursor cleavage- IGF-I gene therapy up-regulated miRNA-186 in the hippocampus of 28 months old female Sprague-Dawley rats. miR-186 is a potent negative regulator of β -site amyloid precursor protein-cleaving enzyme 1 (BACE1) in neuronal cells (see Discussion for further details and references).

Miscellaneous genes downregulated by IGF-I gene therapy in old rats- DUSP1 and Nr4a1 encode for DUSP1 (phosphatase) and Nr4a1 (transcription factor), two proteins induced when the glucocorticoid receptor is phosphorylated and activated.

Taken together, the results of this section show that among the hippocampal genes whose expression was modified by the treatment there is a set of genes functionally relevant to a number of hippocampal activities affected by aging.

DISCUSSION

Cognitive aging leads to a progressive decline in memory function. There is a reduced persistence of experimentally induced, long-term potentiation (LTP) of hippocampal synapses, which is correlated with faster behavioral forgetting of spatial information (21). Spatial memory of aged rats is also impaired as revealed by various tests of spatial learning and

memory (13,22-24). Hippocampal neurogenesis is important for certain types of memory and falls significantly in aged rats (13,25). The present results confirm our previous findings on the restorative ability of IGF-I gene therapy on spatial memory accuracy (7,26).

Gene-expression changes in the hippocampus during aging

There is clear evidence that a constellation of gene expression changes underlie hippocampal phenotype aging. Thus, gene expression studies in aging rodents have documented significant changes in hippocampal genes related to cholesterol synthesis, inflammation, transcription factors, neurogenesis and synaptic plasticity. In rodents, aging and, to a lesser extent, deficits in memory performance have been associated with changes in hippocampal gene expression (8-12). These differences consist mostly of gene upregulation in middle-aged mice (15-mo old) as compared with 2-mo old counterparts (12). In the CA1 hippocampal region of old male rats 233 genes were found to be differentially expressed with aging, 60% upregulated and 40% downregulated (8). We have recently found that in the entire hippocampus of female rats, 210 transcripts are differentially expressed in old animals when compared with young counterparts, with 61% being downregulated and 39% upregulated (27).

Hippocampal transcriptome changes induced by IGF-I gene therapy in old rats

To our knowledge, there are no documented studies on the effects of neuroprotective factor treatment on the hippocampal transcriptome of aging rats. Since we have characterized the restorative effect of IGF-I gene therapy on cognitive performance in aging female rats (7), we were interested in correlating the transcriptome changes induced by long-term IGF-I gene therapy on the hippocampus of aging female rats with hippocampal function improvement. To this end, we performed RNA-seq analysis of the whole female rat hippocampus of old rats ICV

injected with a helper dependent-adenovector expressing rat IGF-I comparing the results with placebo vector-treated counterparts.

From the 219 genes significantly differentially expressed by IGF-I gene therapy in the hippocampus of old rats, we could identify a short list of genes relevant to IGF-I expression and transport, synaptic plasticity and neurogenesis as well as neuronal function.

Genes related to IGF-I- Since our IGF-I adenovector was delivered via ICV, the IGF-I gene upregulation recorded in the hippocampus must reflect the expression of the endogenous rat gene, implying that transgenic IGF-I directly or indirectly stimulated hippocampal IGF-I production. Increased expression of IGF-I in the hippocampus is likely to have played a significant role in the deregulation of a number of hippocampal genes in the experimental old rats (**Fig. 3**). The IGFBP4 and IGFBP6 binding proteins are members of the insulin-like growth factor binding protein family. They bind and prolong life in blood of both insulin-like growth factors (IGFs) I and II and alter their interaction with cell surface receptors (**28,29**).

The treatment downregulated the expression of IGFBP4 and upregulated the expression of IGFBP6. Consequently, hippocampal tissue levels of free IGF-I and IGF-II are likely to have changed as a result of the altered proportion of these two binding proteins.

Genes involved in synaptic plasticity and neurogenesis- Four genes related with synaptic processes and neurogenesis were up-regulated after IGF-I gene therapy, namely Sypl2, Nnat, Itga-8 and DCX.

Sypl2, mouse aliase Mitsugumin 29, is an integral component of synaptic vesicle membrane, it regulates cellular calcium ion homeostasis, transporter activity and substantia nigra development (**30**). Sypl2 is a distinctly inducible gene also in human astrocytes surrounding

A β -containing senile plaques in vivo. In lesions of Alzheimer's Disease (AD) brain, increased expression of Sypl2 is detected only in activated astrocytes. But in quiescent astrocytes in non-AD brain and in lesion-free areas of AD brains, the expression of this gene is controlled at a low level **(31)**. We hypothesize that overexpression of Sypl2 in astrocytes could play a neuroprotective role, preventing the development of senile plaques.

Nnat is a maternal imprinted gene, which encodes a membrane protein in the endoplasmic reticulum **(32,33)**. mRNA levels are highest early in brain development and decrease postnatally **(34)**. However, traces of neuronatin mRNA continue to be present even in the adult brain including the hypothalamus, hippocampus and pituitary gland **(35-37)**. NNAT, shown to be enriched in isolated dendrites, provides a means for rapidly eliciting site-specific changes in protein levels during neuronal development and synaptic plasticity **(35,36,38)**. Importantly, NNAT levels increase during neurogenesis (between E16–19) **(35)**. Oyang and col. reported that NNAT is indeed dendritically translated in mature hippocampal neurons during homeostatic plasticity and that it likely regulates dendritic calcium by modulation of intracellular Ca²⁺ stores by antagonizing SERCA pump activity **(37)**. Although high embryonic and early postnatal expression has suggested significant roles for NNAT during neuronal development and neurogenesis, its function in mature neurons has not been examined. Here, we show that IGF-I up-regulated NNAT in the senile hippocampus, which suggests that this peptide may be playing a significant modulatory role in neuronal plasticity during aging.

A8-integrin (ITGA8) expression in the brain mediates cell-cell interactions and regulates neurite outgrowth of sensory and motor neurons **(39,40)**. Accumulating evidence has implicated integrin function in the CNS physiology underlying synaptic and behavioral plasticity. Mice deficient in α 8-integrin in the forebrain are impaired specifically in the expression of hippocampal LTP **(40)**. In this context, the up-regulation of α 8-integrin in the hippocampus of

senile rats reported here could contribute to restoring LTP and consequently, improve spatial memory.

Doublecortin is a cytoskeleton-associated protein **(41)** present in immature neurons. As such, DCX expression in the hippocampal DG indicates quantity of immature neuron count (neurogenesis). In a previous study, we observed that IGF-I gene therapy prompts an increase in DCX (+) neuron number in the DG of senile rats **(7)**. Thus, the upregulation reported herein is in line with our previous findings.

miRNAs role in aging brain and Alzheimer disease pathology- Studies on the roles that microRNAs (miRNAs) play in brain aging and AD pathogenesis have only recently been initiated **(42-45)**. MiRNAs are endogenous small RNA molecules that control gene expression post-transcriptionally, primarily through binding to complementary target sequences in the 3' untranslated regions (UTRs) of mRNAs. Age is significantly associated with a decline in miRNA expression levels in the brains of fish **(46)**, mice **(45,47,48)**, rats **(49)**, chimpanzees **(44)**, rhesus macaques **(42,44)**, and even humans **(42,44)**. Moreover, low miRNA levels are likely to contribute to loss of brain functioning and neurodegeneration **(50-52)**.

In this context, our finding that IGF-I gene therapy up-regulates miR-186 in the hippocampus of 28 months old female Sprague-Dawley rats is likely to be relevant for improvement of memory function. miR-186 expression is significantly decreased in mouse cortices at 13 months of age, compared to 2 months of age, and it shows a trend to further decrease at 24 months of age. In the brain, miR-186 is broadly expressed across multiple brain subregions in mice **(53)**. miR-186 is a potent negative regulator of β -site amyloid precursor protein-cleaving enzyme 1 (BACE1) in neuronal cells and it may be one of the molecular links between brain aging and the increased risk for AD during aging **(53)**. Importantly, miR-186 over-expression significantly decreases A β level by suppressing BACE1 expression in cells expressing human pathogenic mutant amyloid

precursor protein (**53**). In this context, our finding that IGF-I up-regulates miR-186 levels in the hippocampus of senile rats suggests a neuroprotective role.

Concluding Remarks

The present study shows for the first time, to the best of our knowledge, that IGF-I gene therapy in the brain of aging rats induces significant changes in the expression of a large number of hippocampal genes (219). Although we cannot determine the functional relevance of all of them in hippocampal function, we could identify a limited number of upregulated genes that play a significant role in synaptic plasticity and neurogenesis. Interestingly, IGF-I upregulates the expression of miRNA 186, a micro RNA whose production declines with age and which exerts a neuroprotective action by inhibiting the activity of BACE1 protease. Furthermore, the IGF-I gene and one of its binding proteins were also upregulated. Our results provide an initial glimpse at the molecular mechanisms underlying the neuroprotective actions of IGF-I in the aging brain.

FUNDING

This study was supported by grants #PICT15-0817 and #PICT13-1590 from the Argentine Agency for the Promotion of Science and Technology and grant PIP0597 from the Argentine Research Council (CONICET) to RGG. TFO is supported by the DFG Center for Nanoscale Microscopy and Molecular Physiology of the Brain (CNMPB). MA was supported by grant INC-MSAL. MA, EL, GRM and RGG are career researchers of CONICET. JP is a recipient of a CONICET doctoral fellowship and was supported by a German-Argentine (Ale-Arg) travel fellowship.

OMO is recipient of an IBRO International Fellowship for Postdoctoral Researchers (IBRO/ISN 2015).

ACKNOWLEDGEMENTS

We thank to Dr. Thomas Lingner, University Medical Center, Göttingen, for performing the transcriptome analysis, María José Bellini and Yolanda Sosa for technical assistance as well as to Oscar Vercellini, Araceli Bigres for animal care and to Mario Ramos for assistance with graphics design. TFO is supported by the DFG Center for Nanoscale Microscopy and Molecular Physiology of the Brain (CNMPB).

AUTHORS' CONTRIBUTIONS

JP, GRM and OMO did the cognitive studies and the analysis of the behavioral data. MA, EL, TFO and RGG performed the analysis and interpretation of the RNA-seq data. The qRT-PCR experiments were done by IP. JP, MA and EL designed the different plots and graphs. JP, GRM, MA, EL, TFO and RGG wrote different sections of the manuscript. JP, GRM, TFO and RGG assembled the final version of the paper.

We hereby declare that none of the authors has potential competing interests.

LIST OF ABBREVIATIONS

AD: Alzheimer's disease

AT: acquisition trial

BM: Barnes Maze

CSF: cerebrospinal fluid

DG: dentate gyrus

ICV: intracerebroventricular

IGF-I: Insulin like growth factor I

GO: gene ontology analysis

PT: probe trial

RAd: Recombinant adenoviral vector

REFERENCES

1. Markowska AL, Mooney M, Sonntag WE. Insulin-like growth factor-1 ameliorates age-related behavioral deficits. *Neuroscience*. 1998. 87:559-569.
2. Dore S, Kar S, Quirion R. Insulin-like growth factor-1 protects and rescues hippocampal neurons against amyloid- and amylin-induced toxicity. *Proc nat Acad Sci USA*. 1997. 94: 4772-4777.
3. Carro E, Trejo JL, Gerber A et al. Therapeutic actions of insulin-like growth factor I on APP/PS2 mice with severe brain amyloidosis. 2006. *Neurobiol Aging*. 27:1250-1257.

4. Hereñú CB, Cristina C, Rimoldi OJ, Becú-Villalobos D et al. Restorative effect of Insulin-like Growth Factor-I gene therapy in the hypothalamus of senile rats with dopaminergic dysfunction. 2007. *Gene Ther* 14: 237-245.
5. Hereñú CB, Sonntag WE, Morel GR, Portiansky EL, Goya RG. The ependymal route for insulin like growth factor-1 gene therapy in the brain. 2009. *Neuroscience* 163: 442-447.
6. Nishida F, Morel GR, Hereñú CB, Schwerdt JI, Goya RG, Portiansky EL. Restorative effect of intracerebroventricular Insulin-like Growth Factor-I gene therapy on motor performance in aging rats. 2011. *Neuroscience* 177: 195-206.
7. Pardo J, Uriarte M, Console GM et al. Insulin-like growth factor-I gene therapy increases hippocampal neurogenesis, astrocyte branching and improves spatial memory in aging rats; *European Journal of Neuroscience*. 2016. 44(4):2120-2128.
8. Blalock EM, Chen KC, Sharrow K et al. Gene microarrays in hippocampal aging: statistical profiling identifies novel processes correlated with cognitive impairment. *J Neurosci*. 2003. 23 (9): 3807–19.
9. Burger C, Lopez MC, Feller JA, Baker HV, Muzyczka N, Mandel RJ. Changes in transcription within the CA1 field of the hippocampus are associated with age-related spatial learning impairments. *Neurobiol Learn Mem*. 2007. 87 (1): 21–41.
10. Burger C, Lopez MC, Baker HV, Mandel RJ, Muzyczka N. Genome-wide analysis of aging and learning-related genes in the hippocampal dentate gyrus. *Neurobiol Learn Mem*. 2008. 89 (4): 379–96.
11. Rowe WB, Blalock EM, Chen KC et al. Hippocampal expression analyses reveal selective association of immediate-early, neuroenergetic, and myelinogenic pathways with cognitive impairment in aged rats. *J Neurosci*. 2007. 27 (12): 3098–110.

12. Verbitsky M, Yonan AL, Malleret G, Kandel ER, Gilliam TC, Pavlidis P. Altered hippocampal transcript profile accompanies an age-related spatial memory deficit in mice. *Learn Mem.* 2004. 11 (3): 253–60.
13. Morel GR, Andersen T, Pardo J et al. Cognitive impairment and morphological changes in the dorsal hippocampus of very old female rats. *Neuroscience.* 2015. 303: 189-199.
14. Oka K, Chan L. Helper-dependent adenoviral vectors. *Curr Protoc Hum Genet*;Ch 12:Unit 12.13. (2005).
15. Paxinos G, Watson C. *The rat brain in stereotaxic coordinates.* San Diego: Academic Press. 1998. 154, 2795e2806.
16. Dobin A, Davis CA, Schlesinger F, Drenkow J, Zaleski C, Jha S, Batut P, Chaisson M, Gingeras TR. 2013. STAR: ultrafast universal RNA-seq aligner. *Bioinformatics* 29 :15-21.
17. Li H, Handsaker B, Wysoker A et al. The Sequence Alignment/Map format and SAMtools. 1000 Genome Project Data Processing Subgroup. *Bioinformatics.* 2009. Aug 15;25(16):2078-9.
18. Anders S, Pyl PT, Huber W. HTSeq—a Python framework to work with high-throughput sequencing data. *Bioinformatics.* 2015. 31:166-9.
19. Robinson, MD, McCarthy, DJ, Smyth, GK (2010). edgeR: a Bioconductor package for differential expression analysis of digital gene expression data. *Bioinformatics* 26, 139–140.
20. Saeed AI, Sharov V, White J et al. TM4: a free, open-source system for microarray data management and analysis. *Biotechniques.* 2003. 34:374–378.
21. Barnes CA, McNaughton BL. An age comparison of the rates of acquisition and forgetting of spatial information in relation to long-term enhancement of hippocampal synapses. *Behav Neurosci.* 1985. 99: 1040–1048.

22. de Toledo-Morrell L, Morrell F, Fleming S. Age-dependent deficits in spatial memory are related to impaired hippocampal kindling. *Behav Neurosci.* 1984. 98 :902-90.
23. Morris R. Developments of a water-maze procedure for studying spatial learning in the rat. *J Neurosci Meth.* 1984. 11: 47–60.
24. Barnes CA. Memory deficits associated with senescence: a neurophysiological and behavioral study in the rat *J Comp Physiol Psychol.* 1979. 93: 74–104.
25. Lichtenwalner RJ, Forbes ME, Bennett SA et al. Intracerebroventricular infusion of insulin-like growth factor-I ameliorates the age-related decline in hippocampal neurogenesis. 2001. *Neuroscience.* 107. 603–613.
26. Morel GR, Lopez-Leon M, Uriarte M, Reggiani PC, Goya RG; Therapeutic potential of IGF-I on hippocampal neurogenesis and function during aging. *Neurogenesis.* 2016 Dec 20;4(1).
27. Pardo J, Abba M, Lacunza E et al. Identification of a conserved gene signature associated with an exacerbated inflammatory environment in the hippocampus of aging rats. 2017. *Apr;27(4):435-449*
28. Shimasaki S, Uchiyama F, Shimonaka M, Ling N. Molecular cloning of the cDNAs encoding a novel insulin-like growth factor-binding protein from rat and human. *Mol Endocrinol.* 1990. Oct;4(10):1451-8.
29. Ehrenborg E, Zazzi H, Lagercrantz S et al. Characterization and chromosomal localization of the human insulin-like growth factor-binding protein 6 gene. *Mamm Genome.* 1999. Apr;10(4):376-80.
30. Shimuta M, Komazaki S, Nishi M, Iino M, Nakagawara K, Takeshima H. Structure and expression of mitsugumin29 gene. *FEBS Lett.* 1998. 431, 263–267.



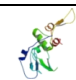



31. Satoh K, Akatsu H, Yamamoto T, Kosaka K, Yokota H, Yamada T. Mitsugumin 29 is transcriptionally induced in senile plaque-associated astrocytes. *Brain Res.* 2012 Mar 2;1441:9-16.
32. Dou D, Joseph R. Cloning of human neuronatin gene and its localization to chromosome-20q 11.2–12: the deduced protein is a novel ‘‘proteolipid’’. *Brain Res.* 1996. 723: 8–22.
33. Kagitani F, Kuroiwa Y, Wakana S et al. Peg5/Neuronatin is an imprinted gene located on sub-distal chromosome 2 in the mouse. *Nucleic Acids Res.* 1997. 25: 3428–3432.
34. Poon MM, Choi SH, Jamieson CA, Geschwind DH, Martin KC. Identification of process-localized mRNAs from cultured rodent hippocampal neurons. *J Neurosci.* 2006. 26: 13390–13399.
35. Joseph R, Dou D, Tsang W. Neuronatin mRNA: alternatively spliced forms of a novel brain-specific mammalian developmental gene. *Brain Res.* 1995. 690: 92–98.
36. Usui K, Morii R, Tanaka R et al. cDNA cloning and mRNA expression analysis of the human neuronatin. High level expression in human pituitary gland and pituitary adenomas, *J Mol Neurosci.* 1997. 9 55–60.
37. Oyang EL, Davidson BC, Lee W, Poon MM. Functional characterization of the dendritically localized mRNA neuronatin in hippocampal neurons. *PLoS One.* 2011. 6(9):e24879.
38. Joseph R, Dou D, Tsang W. Molecular cloning of a novel mRNA (neuronatin) that is highly expressed in neonatal mammalian brain. *Biochem Biophys Res Commun.* 1994. 201:1227–1234.
39. Bossy B, Bossy-Wetzler E, Reichardt LF. Characterization of the integrin $\alpha 8$ subunit: a new integrin $\beta 1$ -associated subunit, which is prominently expressed on axons and on cells in contact with basal laminae in chick embryos. *EMBO J.* 1991. 10:2375–2385.

40. Chan C-S, Chen H, Bradley A, Dragatus I, Rosenmund C, Davis RL. α 8-integrins are required for Hippocampal Long-Term Potentiation but not for Hippocampal-Dependent Learning. *Genes, brain, and behavior*. 2010. 9(4):402-410.
41. Gleeson JG, Lin PT, Flanagan LA, Walsh CA. Doublecortin is a microtubule associated protein and is expressed widely by migrating neurons. *Neuron*. 1999. 23:257–271.
42. Somel M, Guo S, Fu N, Yan Z, et al. MicroRNA, mRNA, and protein expression link development and aging in human and macaque brain. *Genome Res*. 2010. 20(9): 1207–1218.
43. Eda A., Takahashi M., Fukushima T, Hohjoh H. Alteration of microRNA expression in the process of mouse brain growth. *Gene*. 2011. 485, 46–52.
44. Persengiev S, Kondova I, Otting N, Koeppen A H, Bontrop RE. Genome-wide analysis of miRNA expression reveals a potential role for miR-144 in brain aging and spinocerebellar ataxia pathogenesis. *Neurobiol. Aging*. 2011. 32(2316), e2317–e2327.
45. Inukai S, de Lencastre A, Turner M, Slack F. Novel microRNAs differentially expressed during aging in the mouse brain. *PLoS ONE*. 2012. 7, e40028.
46. Baumgart M, Groth M, Priebe S et al. Age-dependent regulation of tumor-related microRNAs in the brain of the annual fish *Nothobranchius furzeri*. *Mech. Ageing Dev*. 2012. 133(5):226-33.
47. Cheng XR, Cui XL, Zheng Y et al. Nodes and biological processes identified on the basis of network analysis in the brain of the senescence accelerated mice as an Alzheimer's disease animal model. *Front. Aging Neurosci*. 2013. 29;5:65.
48. Li X, Khanna A, Li N, Wang E. Circulatory miR34a as an RNAbased, noninvasive biomarker for brain aging. *Aging*. 2011. 3(10):985-1002.

49. Rao YS, Mott NN, Wang Y, Chung WC, Pak TR. MicroRNAs in the aging female brain: a putative mechanism for age-specific estrogen effects. *Endocrinology*. 2013. 154(8):2795-806.
50. Abe M, Bonini NM. MicroRNAs and neurodegeneration: role and impact. *Trends Cell Biol*. 2013. 23(1):30-6.
51. Lau P, Bossers K, Janky R et al. Alteration of the microRNA network during the progression of Alzheimer's disease. *EMBO Mol. Med*.2013. 5(10):1613-34.
52. Persengiev SP, Kondova II, Bontrop RE. The impact of microRNAs on brain aging and neurodegeneration. *Curr. Gerontol. Geriatr. Res*. 2012. 2012:359369.
53. Kim J, Yoon H, Chung DE, Brown JL, Belmonte KC, Kim J. miR-186 is decreased in aged brain and suppresses BACE1 expression *Journal of neurochemistry*. 2016. 137 :436–445.

Table 1

Effect of IGF-I gene therapy on functionally relevant hippocampal genes of old rats

Gene	Biological function	Expression modulation	Reference
Igf1 	Neuroprotection	↑	<i>Pardo et al., 2016</i>
Dcx 	Neurogenesis	↑	<i>Gleeson et al., 1999</i>
Itga8	Cell-cell interaction	↑↑↑	<i>Bossy et al., 1991; Chan et al., 2010</i>
Sypl2	Synaptic function	↑↑	<i>Shimuta et al., 1998</i>
Nnat		↑↑	<i>Dou et al., 1996; Kagitani et al., 1997</i>
Igfbp4 	IGF transport in blood	↓	<i>Shimazaki et al., 1990</i>
Igfbp6 		↑	<i>Ehrenborg et al., 1999</i>
Ang2 	Blood vessel growth	↓↓	<i>Yuan et al., 2009</i>
Dusp1	Glucocorticoid response	↓↓	<i>Arango-Lievano et al., 2016</i>
Nr4a1		↓	
MiRNA 	β-Amyloid processing	↑	<i>Kim et al., 2016</i>

The indicated references are included in the general Reference list at the end of the paper. The number of arrows for each gene indicates the magnitude of its deregulation in the old rats of the IGF-I group versus the DsRed counterparts.

FIGURE LEGENDS

Figure 1. Effect of IGF-I gene therapy on the performance of old rats in the Barnes Maze.-

Panel A, shows a diagram illustrating the experimental design used. Learning ability was assessed by performing 3 sessions of 9 days each (4 AT per day) with a 30-day interval between each session. On the last day of each session a probe trial (PT) was conducted. DsRed or IGF-I adenovectors were ICV injected on Experimental Day 0 (syringe icon). Eut= Euthanize. **Panels B and C** show latency to escape hole and error number during the three sessions performed during the experiment. Arrows indicate vector injection day. **Panels D, E and F** show hole exploration frequency in probe trials 1, 2 and 3. Notice the sharp increase in exploratory frequency of hole #0 (escape hole) in the IGF-I group at PT3. Data are represented as mean \pm SEM. Comparisons between IGF-I versus DsRed are made for each pair of IGF-I – DsRed time points. *: $P < 0.05$. N was 10 for DsRed group and 12 for IGF-I group.

Figure 2. Transgene expression and IGF-I levels in the CSF of DsRed and IGF-I rats. Panel A

shows a brightfield image of the LV of an old rat 2 days after DsRed adenovector injection. **Panel B** shows expression (red fluorescence) of DsRed in the ependymal layer of the LV. **Panel C** represents a magnification of the yellow framed region shown on Panel B. **Panel D** shows a diagrammatic representation of the ependymal cell layer shown on Panel C. **Panels E, F and G** show DsRed fluorescence, DAPI staining and merge of the two colors, respectively, in the 3V at the end of the experiment (Exp. Day 80). **Panel H** shows CSF IGF-I levels on Exptl. day 80 in DsRed and IGF-I animals. N was 3 and 4 for the DsRed and IGF-I groups, respectively. LV, lateral ventricle; 3V, third ventricle; CPu, caudate putamen. Scale bar for panel B=250 μ m which also applies to panel A; scale bar for panel G=100 μ m which also applies to panels C, E, and F.

Figure 3. **A.** Heatmap representation of the 219 DEG (138 up & 81 down) genes between DsRed and IGF-I rats ordered according to the LogFC values. **B.** Functional enrichment of the upmodulated genes in IGF-I rats, based on Kegg-2016 gene set library. **C.** Network representation of IGF-I related genes obtained from the list of upmodulated genes. Red nodes indicate genes from the query gene list, whereas blue nodes indicates genes related to the query. **D.** Bar plots representing qRT-PCR of four representative genes induced and repressed by IGF-I gene therapy: N=4 for both groups. Bars represent mean \pm SD. * $p < 0.05$, ** $p < 0.01$, *** $p < 0.001$.

Figure 1

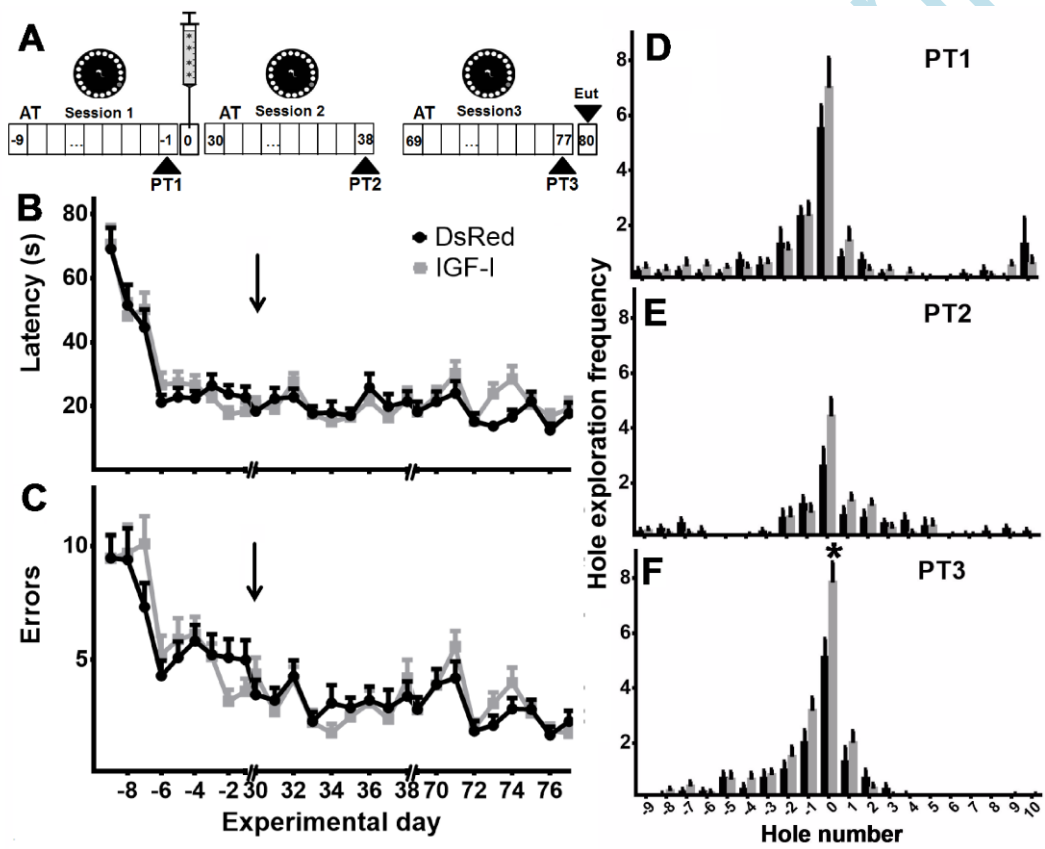


Figure 2

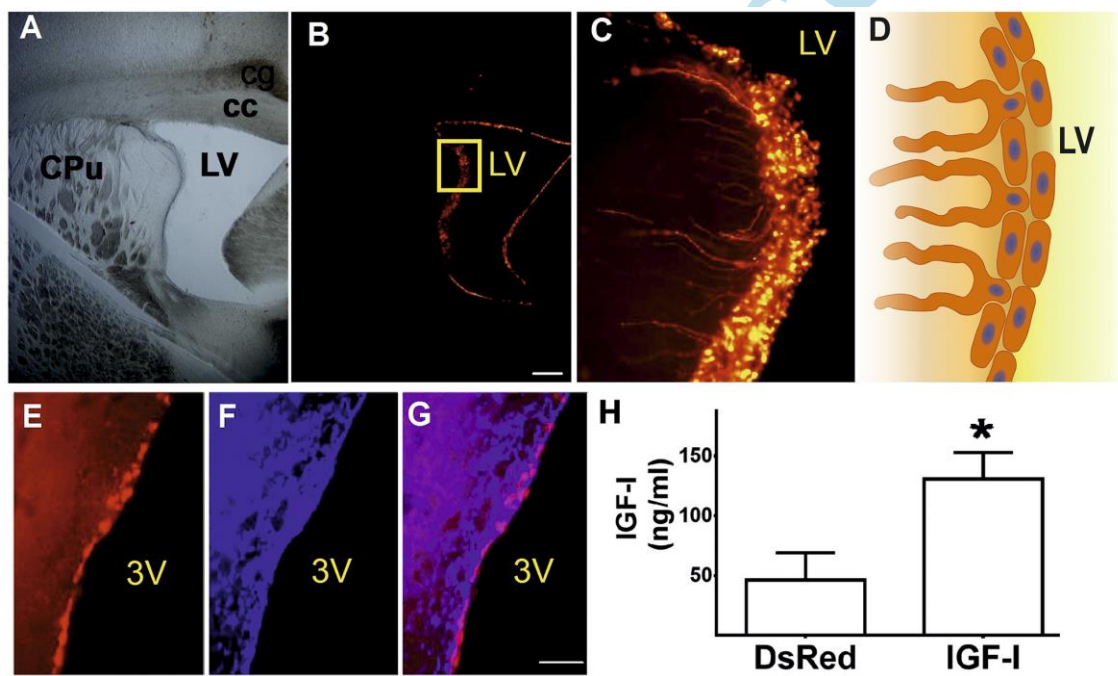


Figure 3

